



Highly alloyed PtRu black electrocatalysts for methanol oxidation prepared using magnesia nanoparticles as sacrificial templates



Liangliang Zou ^{a,b}, Jing Guo ^a, Juanying Liu ^a, Zhiqing Zou ^a, Daniel L. Akins ^c, Hui Yang ^{a,*}

^a Shanghai Advanced Research Institute, Chinese Academy of Sciences (CAS), Shanghai 201210, China

^b University of the CAS, Beijing 100039, China

^c CASI and the Chemistry Department of The City College of New York, CUNY, 10031, USA

HIGHLIGHTS

- Magnesia is used as a sacrificial support for the synthesis of PtRu black catalyst.
- The PtRu black electrocatalysts show high alloying degree and small particle size.
- Catalytic activity for MeOH oxidation is ca. twice that of commercial PtRu black.
- In-house PtRu black catalysts have enhanced durability over commercial catalysts.

ARTICLE INFO

Article history:

Received 28 July 2013

Received in revised form

16 September 2013

Accepted 18 September 2013

Available online 30 September 2013

Keywords:

Platinum–ruthenium black

Alloying

Methanol oxidation

Direct methanol fuel cell

ABSTRACT

Synthesis of small particle size, highly alloyed PtRu black catalysts for application in direct methanol fuel cells remains a substantial challenge. In this work, PtRu (1:1) black catalysts have been synthesized using Pt carbonyl complex and RuCl₃ as initial precursors and magnesia nanoparticles as sacrificial templates. Magnesia is used to prevent the aggregation of synthesized PtRu nanoparticles during heat treatment, and thus promoting the controllable formation of PtRu black of high alloy composition and small particle size. X-ray diffraction shows that the PtRu black nanoparticles have a single-phase face-centered cubic structure and that the degree of alloying increases with treatment temperature. The mean particle size of the PtRu black catalysts, after heat-treatment from 250 to 300 °C, is found to be ca. 3 nm, only slightly larger than that of commercial Johnson-Matthey PtRu black, but more highly alloyed. Electrochemical measurements indicate that the catalytic activity for methanol oxidation on in-house prepared PtRu black catalysts is about twice that of the commercial product, with greater durability, indicating that the degree of alloying between Pt and Ru plays an important role in improving both catalytic activity and durability of the catalysts when used for methanol oxidation.

© 2013 Elsevier B.V. All rights reserved.

1. Introduction

PtRu-based catalysts are regarded generally as the most suitable anode catalysts for direct methanol fuel cells (DMFCs) because they can completely oxidize methanol to CO₂ via a rapid, two-step mechanism. This mechanism involves (CO)_{ad} on the Pt site reacting with (OH)_{ad} on a neighboring Ru site. The electrocatalytic activity is therefore strongly dependent on the distribution of Pt and Ru sites at the atomic level [1,2]. Until recently, much effort has been devoted to the synthesis of bimetallic PtRu nanoparticles on various supports such as carbon materials [3–5], metal oxide

modified carbon materials [6] and transition metal oxides [7,8]; with the best Pt:Ru ratio typically reported to be 1:1. However, for practical applications, it is highly desirable to reduce the thickness of the catalytic layer to improve mass transportation and to decrease the inner electrical resistance. As a result, PtRu catalysts with high metal loading or even unsupported PtRu black have been extensively used in the DMFCs [9,10]. However, synthesis of PtRu black catalysts of higher catalytic activity, greater alloy percentage, with more uniform nanoparticle size distribution, and not requiring a support remains an enormous challenge.

There are only a few reports that focus on the synthesis of PtRu black catalyst, likely due to the conflict of the desired small particle size and high alloy composition. Moreover, there are only a few reports in the literature dealing with the important role that alloy extent plays in the electrocatalytic activity and stability of PtRu

* Corresponding author. Fax: +86 21 20325112.

E-mail addresses: yangh@sari.ac.cn, huiyang65@hotmail.com (H. Yang).

nancatalysts used for methanol oxidation [11]. Usually, PtRu nanoparticles of high alloy composition are prepared at high temperature. However, the average size of the PtRu particles prepared at high temperature is generally large with high crystallinity, leading to an insufficient electrocatalytic activity. As an example, Gilman et al. [12] synthesized PtRu black catalyst by the decomposition of metallic chlorides and chloroacids. The alloy composition was well controlled, but the particle size varied between 13.3 and 61.5 nm, while the Ru content decreased from 73% to 15%. Also, Guo et al. [13] used a modified polyol process to synthesize PtRu black, which was found to have a mean particle size of ca. 2.6 nm. But, the amount of alloyed Pt and Ru was extremely low. Additionally, Korzeniewski et al. [14–16] recently synthesized nanosized PtRu black catalysts of controlled Pt and Ru alloy content via a sonochemical approach, but the PtRu black catalysts, despite having high alloy compositions, exhibited low catalytic activity for methanol oxidation.

However, there are complex routes that use a small molecule as surfactants—which are easy to remove through rinsing—that lead to a fine control over the alloy composition [17–19]. And, according to Dickinson et al. [20], Pt carbonyl and Ru carbonyl compounds can produce supported PtRu catalyst for methanol oxidation in one step; however, there are presently no reports on the synthesis of unsupported PtRu black catalysts (by a complex route) for the DMFC.

In the present work, magnesia (MgO), a cheap metal oxide, is employed as a sacrificial support in a complex synthesis that results in the formation of PtRu nanoparticles of high alloy composition. Subsequent removal of magnesia yields PtRu black nanoparticles. Additionally, the tuning of size and alloy content of the PtRu nanoparticles has been investigated by adjusting the MgO/Pt mass ratio and the heat treatment temperature. The catalysts' microstructures and activities have been characterized and compared with commercial PtRu black by X-ray diffraction (XRD), transmission electron microscopy (TEM), X-ray photoelectron spectroscopy analysis (XPS) and electrochemical measurements.

2. Experimental

2.1. Materials

All reactants were used as received. Sinopharm Chemical Reagent Co., Ltd., supplied sodium acetate (CH_3COONa), magnesia (MgO), methanol (CH_3OH , AR), and ruthenium chloride (RuCl_3). Sodium chloroplatinate ($\text{Na}_2\text{PtCl}_6 \cdot 6\text{H}_2\text{O}$) was purchased from Aldrich. Commercial PtRu was supplied by Johnson Matthey. Ultrapure water (18.2 $\text{M}\Omega \text{ cm}$) was used both for solution preparation and for washing.

2.2. Preparation of platinum ruthenium black nanocatalysts

A carbonyl complex route was employed to prepared nanosized platinum–ruthenium black catalysts. For example, Pt–carbonyl complexes were synthesized using methanol as a solvent through the reaction of Na_2PtCl_6 with CO at about 50 °C for 24 h, with constant mechanical stirring [19–22], and with a NaAC/Pt molar ratio of 7.2. After the synthesis of Pt carbonyls, a stoichiometric amount of RuCl_3 and a small amount of MgO were added to the mixture under N_2 gas flow, and the mixture was stirred at about 55 °C for more than 6 h. Subsequently, the solvent was removed and the powder was subjected to heat treatment at different temperatures ranging from 250 °C to 300 °C under hydrogen/nitrogen for 2 h. After heat treatment, the sample was dispersed in 50 mL H_2SO_4 solution and stirred for 5 h to remove the MgO template material; then washed with water until no chlorine ions

were detected in the supernatant; the resultant product was then dried.

The PtRu black catalyst is denoted as PtRu- x - y , where x stands for different MgO/Pt mass ratio when y is the heat-treatment temperature. For example, the PtRu black catalyst prepared with MgO/Pt mass ratio of 4 and heat-treated temperature at 250 °C is named PtRu-4-250 °C.

2.3. Physical characterization

An IRIS advantage inductively coupled plasma; atomic emission spectroscopy (ICP-AES) system (Thermo America) was employed to analyze the composition of the catalysts. Powder X-ray diffraction (XRD) measurements were conducted using a Bruker AXS D8 Advance powder X-ray diffractometer with a Cu K α ($\lambda = 1.5418 \text{ \AA}$) radiation source, operating at 40 kV and 40 mA. Diffraction patterns were collected with a scanning rate of 2° min^{-1} and with a step size of 0.02° . Transmission electron microscopy (TEM) images were obtained with a JEOL 2100F at an accelerating voltage of 200 kV. Prior to observation, after heat treatment, the powder was sonicated in a 0.5 M H_2SO_4 solution with 1 M polyvinyl pyrrolidone (PVP) for 10 min, and then dropped onto a holey carbon film supported on a copper grid. X-ray photoelectron spectroscopy was carried out using a Kratos AXIS Ultra^{DLD} with Al K α radiation. The binding energies derived from XPS measurements have been referenced to the C1s binding energy at 284.45 eV.

2.4. Electrochemical characterization

Porous electrodes were prepared as described previously [19,23]. Briefly, 10 mg of catalysts, 2.5 mL of water, and 0.5 mL of Nafion solution (5 wt. %, Aldrich) were mixed ultrasonically. A measured volume (ca. 3 μL) of this ink was transferred onto a freshly polished glassy carbon disk (GC, 3 mm in diameter), and left to dry overnight at room temperature. Electrochemical measurements (all conducted at 25 ± 1 °C) were performed using a CHI 730B Potentiostat and a conventional three-electrode electrochemical cell. The counter electrode was a glassy carbon plate, and a saturated calomel electrode (SCE) was used as the reference electrode. Potentials quoted herein are with respect to RHE. The electrolyte used was 0.5 M H_2SO_4 or 0.5 M $\text{CH}_3\text{OH} + 0.5 \text{ M H}_2\text{SO}_4$ solution. The real surface areas of all the catalysts were determined by CO_{ad} oxidation in CO stripping voltammetry. The oxidation charge for a monolayer of adsorbed CO on a Pt surface is assumed to be $420 \mu\text{Ccm}^{-2}$ [24]. High-purity nitrogen was used for deaeration of the solutions, and during measurements a nitrogen flow was maintained above the electrolyte solution.

Membrane electrode assembly (MEA) for the DMFC was fabricated by hot-pressing (130 °C, 6 MPa) a pre-treated Nafion-115 membrane sandwiched between anode and cathode for 3 min [23]. In the case of anode, an ink including PtRu black catalysts and 20 wt. % Nafion was blade-coated on the surface of anodic micro-porous layer (MPL) which was formed by spraying a comprising of VXC-72 carbon and 20 wt. % PTFE on the carbon paper. The metal loading of the electrode is ca. 4 mg cm^{-2} . The cathode was prepared with the same procedure as the anode except the catalysts was Pt black (JM) and the MPL carbon content on the carbon cloth, instead of carbon paper, was 2 mg cm^{-2} while the anode's was 1 mg cm^{-2} . The polarization curves of the MEAs were obtained on an Arbin FCT system (Arbin Inc., USA) at a temperature of ca. 25 °C and under ambient atmosphere. 3 M of methanol solution was injected into anode reservoir and the cathode was operated under air-breathing mode for each discharging current point along the polarization curve. A period of 2 min waiting time was used to obtain the stable voltage.

3. Results and discussion

3.1. Physical characterization of PtRu black catalysts

The results of ICP-AES analysis indicate that the compositions of the PtRu black catalysts are very close to the stoichiometric values, which indicating that Pt and Ru are co-reduced and that Ru can be alloyed with Pt via such a synthesis approach.

Fig. 1 shows the XRD patterns of the in-house prepared PtRu black of different MgO/Pt mass ratios at heat-treatment temperature of 250 °C; for the sake of comparison, the XRD pattern for PtRu-JM black is also shown in the figure. All the XRD patterns clearly show five main characteristic peaks of face-centered-cubic (fcc) crystalline Pt, namely, the planes (111), (200), (220), (311) and (222), demonstrating that all the catalysts are mainly single-phase, with a fcc disorder structure (i.e., solid solutions) [19,25]. The diffraction peaks are at higher angles in all PtRu black relative to pure Pt, probably indicating the formation of alloy between Pt and Ru. Also there are no peaks for pure Ru and its oxides found in all PtRu black catalysts. **Fig. 1B** shows XRD patterns of PtRu black with MgO/Pt mass ratio of 4 and heat-treated at various temperatures, which also display five main diffraction peaks. With increase of the heat-treatment temperature, these diffraction peaks shift to higher angles in in-house prepared PtRu black compared to commercial PtRu black, which can be clearly seen in **Fig. 1C**, revealing higher alloy degree of in-house prepared PtRu black than commercial PtRu black. Also, such angle shifts reveal alloy formation between Pt and Ru which indicates that substitution of ruthenium atoms into the platinum lattice leads to decrease lattice parameters and the enhancement of alloy degree with the heating temperature rising.

The calculated lattice parameters (a_{fcc}) for the PtRu black catalysts, which reflect the formation of the solid solution, using the (220) crystal faces, are provided in **Tables 1 and 2**. The alloying degree of the PtRu black catalyst is defined as the Ru atomic fraction (χ_{Ru}) in the PtRu alloy, which is related to the lattice parameter by the following equation proposed by Antolini et al. [26]:

$$\alpha = \alpha_0 - 0.124\chi_{\text{Ru}} \quad (1)$$

Where α is the lattice parameter of PtRu black and α_0 is the lattice parameters of Pt (with the value of 0.3915 nm). The results obtained are also listed in **Tables 1 and 2**. From the tables, the alloy composition of PtRu-JM is 0.36, which is similar to Stoupin's XRD results [16]. The alloy composition of the in-house prepared PtRu black is found to decrease with MgO/Pt mass ratio increase. Also, with increase of the heat treatment temperature in the condition of MgO/Pt mass ratio of 4, χ_{Ru} is found to increase and reach to the value 0.47 (note that the theoretical maximum value is 0.5). These results suggest that PtRu black synthesized by our method results in high alloy compositions.

The mean particle size of the PtRu black catalysts is calculated using the Scherrer equation based on the X-ray peak width of the (220) reflection. The particle sizes for different catalysts are also provided in **Tables 1 and 2**. The mean particle size obtained for the in-house prepared PtRu-2-250 °C is 3.32 nm and the mean particle size of the catalysts decreases when the value of MgO/Pt increases. However, the mean particle size of the catalyst changed only slightly when the value of MgO/Pt increases from 4 to 8. **Fig. 2** shows a typical TEM image of the PtRu black catalyst with MgO/Pt mass ratio of 4 after heat-treatment at 300 °C and its corresponding particle size distribution histogram. The PtRu black catalysts nanoparticles have a narrow particle size distribution. Based on randomly chosen particles size analysis in the TEM images, the mean particle sizes of the in-house prepared PtRu alloy catalysts

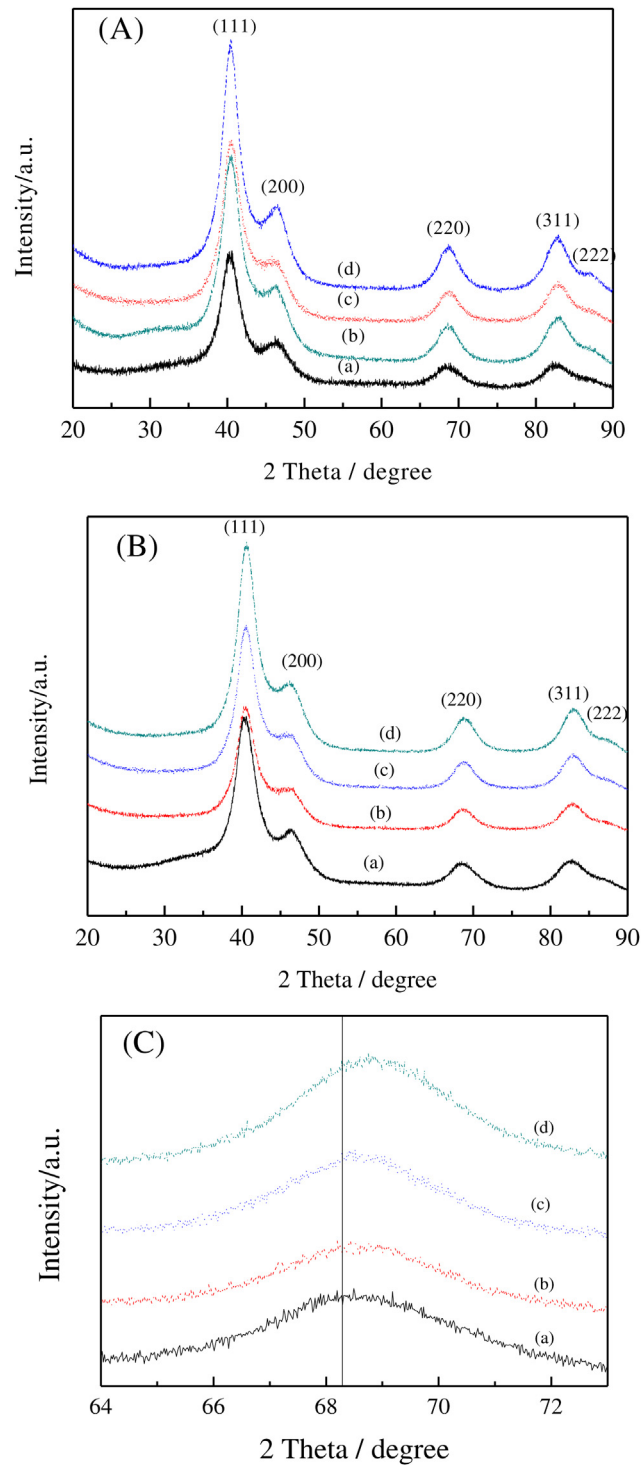


Fig. 1. XRD patterns of the (A) PtRu black catalysts with different MgO/Pt mass ratio (a) PtRu-JM, (b) PtRu-8-250 °C, (c) PtRu-4-250 °C, and (d) PtRu-2-250 °C; (B) PtRu black with MgO/Pt mass ratio of 4 heat-treatment at different temperatures (a) PtRu-JM, (b) 250 °C, (c) 275 °C, and (d) 300 °C (C) enlarged corresponding PtRu black catalysts in (B) (220) diffraction plane.

with MgO/Pt mass ratio of 4 heat-treated at 250, 275 and 300 °C are 2.75, 2.92 and 3.11 nm, respectively. The values are in good agreement with the XRD results. The ascertained mean particle size is small for PtRu black catalysts, which may be beneficial for an increase in the methanol oxidation activity. Hence, the catalyst preparation procedure via the complex approach may be a suitable

Table 1

Structural parameter and particle size of the PtRu black catalysts at different MgO/Pt mass ratio and the PtRu black (Johnson-Matthey) catalyst.

Catalyst	Lattice parameter/nm	Particle size from XRD/nm	χ_{Ru}
PtRu-2-250 °C	0.3863	3.32	0.42
PtRu-4-250 °C	0.3865	2.81	0.40
PtRu-8-250 °C	0.3866	2.80	0.39
PtRu-JM	0.3870	2.72	0.36

method for obtaining catalysts with high alloy extent and narrow size distribution.

Three typical PtRu black catalysts and commercial samples are subjected to XPS analysis to explore the electronic properties and surface composition of the PtRu black catalysts. Fig. 3A displays the Pt 4f XPS spectra of PtRu black catalysts, the in-house prepared PtRu black catalysts showing two peaks for each located at ca. 71.4 and 74.8 eV (solid lined in the figure). The observed binding energies are very close to those of the commercial PtRu black catalyst's and the bulk Pt which are respectively 71.2 and 74.5 eV (dashed lines in the figure) for Pt 4f7/2 and Pt 4f5/2, and much lower than those of Pt oxide [27]. The slightly higher binding energies would lead to weaker adsorption of the poisoning CO species for Pt within the bimetallic catalysts, which would lead to a decrease in the poisoning effect and improve the catalytic activity [28]. We did not find an obvious change in Pt4f binding energies of in-house prepared PtRu black catalysts with increase in the heat treatment temperature, indicating that these samples' microenvironments may be very similar [29]. Because the Ru3d peak ($3d_3/2 = 284.3$ eV) is similar with the C 1s peak ($1s = 284.5$ eV), the oxidation states of Ru in the catalysts was analyzed on Ru 3p peaks. Fig. 3B shows the Ru 3p_{3/2} sections of XPS spectra of PtRu black catalysts. It can be determined that the binding energies of Ru 3p_{3/2} in the PtRu-JM, PtRu-4-250 °C, PtRu-4-275 °C and PtRu-4-300 °C catalysts are 462.4, 462.1, 461.8 and 461.6 eV, respectively. A typical XPS spectrum in the Ru 3p region is deconvoluted into two peaks using the software XPS-Peak of PtRu-4-250 °C catalyst to determine the proportions of metal in various oxidation states (Fig. 3C). The binding energies of the two peaks are ca. 461.7 and 463.9 eV, assigned as Ru(0) metal and Ru(IV)(e.g., RuO₂), respectively. The respective proportions of Ru(0) and Ru(IV) on the surface are 64.7% and 35.3% and the proportions of Ru(0) is 56.4% for PtRu-JM, 65.5% for PtRu-4-275 °C, and 65.6% for PtRu-4-300 °C, respectively. The higher proportion of Ru(0) may lead to a higher electrooxidation activity for methanol [30].

3.2. Electrochemical characterization of the PtRu black catalysts

Fig. 4 shows CO stripping voltammograms of the PtRu black catalysts with a MgO/Pt mass ratio of 4. Compared with the Pt black catalyst with the CO oxidation peak at 0.80 V/RHE, all of the PtRu black catalysts show negative shifts of oxidation peaks, indicating the enhanced activity associated with addition of Ru to Pt. The onset CO-oxidation potential, CO-oxidation peak potential and real

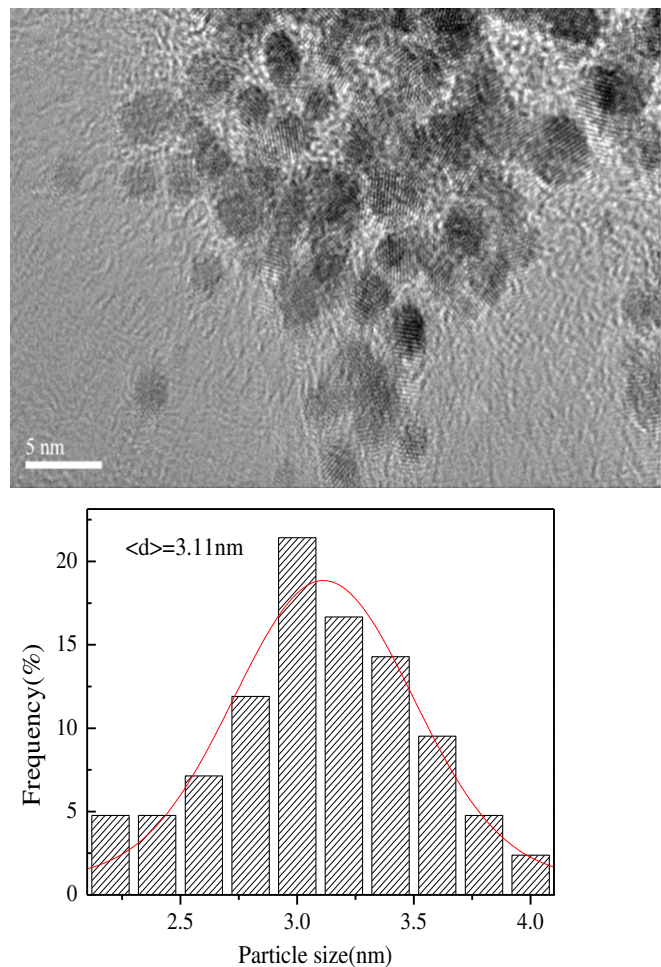


Fig. 2. A typical TEM image of PtRu black with MgO/Pt mass ratio of 4 after heat-treatment at 300 °C.

surface area of PtRu black catalysts are listed in Table 2. It can be seen that the real surface area of the PtRu-JM black catalyst is larger than all in-house prepared PtRu black catalysts, which may be attributed to the smaller particle size of the PtRu-JM black catalysts. The real surface area of Pt within the in-house prepared PtRu black catalysts decreases with increase in the heat treatment temperature. It is clear that with the increase of heat treatment temperature, the onset and peak potentials of the (CO)_{ad} oxidation are shifted to more negative potentials, suggesting that Pt–Ru alloy with high alloying extent is formed and the CO tolerance increases in the order of PtRu-JM < PtRu-4-250 °C < PtRu-4-275 °C < PtRu-4-300 °C, probably due to the effect of the Ru/Pt composition of the catalysts. It can be deduced that the stripping peak potential shifts negatively with increase in the amount of alloy formed in the PtRu black catalyst, which agrees with the XRD results. In the literature,

Table 2

Structural parameter and electrochemical results of the PtRu black catalysts heat-treatment at different temperatures with MgO/Pt mass ratio of 4 and the PtRu black (Johnson-Matthey) catalyst.

Catalyst	Lattice parameter/nm	Particle size from XRD/nm	χ_{Ru}	CO oxidation onset potential/V	CO oxidation peak potential/V	$\text{ESCAco}/\text{m}^2 \text{ g}^{-1}$	Peak current of MOR/mA mg ⁻¹
PtRu-4-300 °C	0.3857	3.10	0.47	0.4431	0.502	19.89	164
PtRu-4-275 °C	0.3861	2.97	0.44	0.4485	0.515	21.53	177
PtRu-4-250 °C	0.3865	2.81	0.40	0.4562	0.524	23.72	198
PtRu-JM	0.3870	2.72	0.36	0.4613	0.511	27.20	91

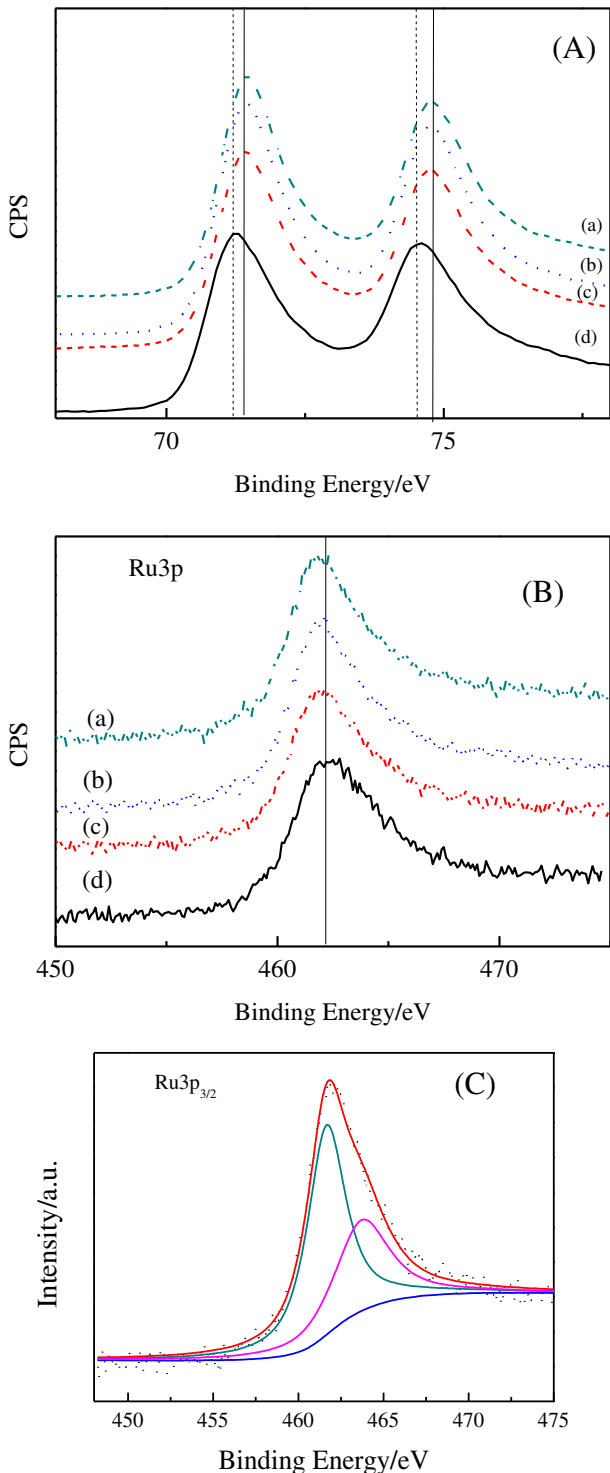


Fig. 3. XPS spectra of in-house prepared PtRu black heat-treatment at different temperatures (a) PtRu-4-300 °C, (b) PtRu-4-275 °C, (c) PtRu-4-250 °C, and (d) PtRu-JM in the binding energy ranges of (A) Pt 4f, (B) Ru 3p, and (C) Ru 3p of PtRu black heat-treatment at 250 °C.

other investigators have discussed the effect of the alloying extent of Pt and Ru on the electrocatalytic activity of Pt–Ru catalysts for methanol oxidation [11]. It is suggested that the high Pt–Ru alloy composition results in improved methanol oxidation due to weaken adsorption of CO (one of the intermediates of the methanol oxidation that is strongly adsorbed on Pt) on the PtRu catalyst and diminished poisoning of the Pt catalyst [31,32].

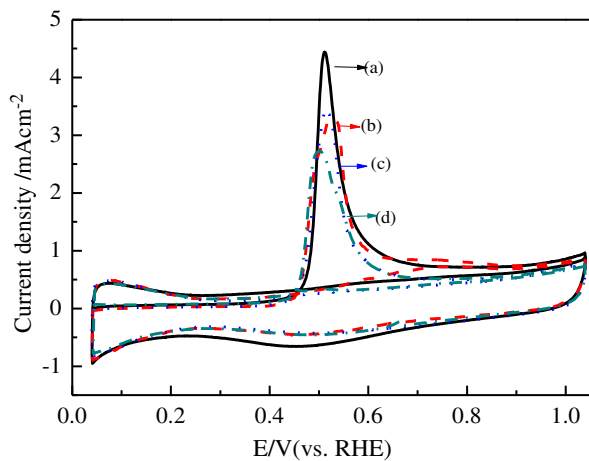


Fig. 4. CO-stripping voltammograms of the (a) PtRu-JM, (b) PtRu-4-250 °C, (c) PtRu-4-275 °C, and (d) PtRu-4-300 °C at a scan rate of 20 mV s⁻¹ in 0.5 M H₂SO₄.

Cyclic voltammetry was used to evaluate and benchmark the activities of PtRu black catalysts. Fig. 5 is a comparison of methanol oxidation using the PtRu black catalysts prepared with different MgO/Pt mass ratio and heat treatment at 250 °C, as well as that for the commercial PtRu black catalyst; all measurement were acquired at a scan rate of 20 mV s⁻¹ in 0.5 M CH₃OH + 0.5 M H₂SO₄. The peak current densities of methanol oxidation on the PtRu black catalysts decrease in the order of PtRu-4-250 °C > PtRu-8-250 °C > PtRu-JM > PtRu-2-250 °C, indicating that the PtRu black with MgO/Pt mass ratio of 4 has the highest methanol oxidation activity. Moreover, the PtRu-2-250 °C showed the lowest methanol oxidation activity (possibly due to aggregation of the PtRu nanoparticles) and largest mean particle size. The activity of PtRu-8-250 °C was lower than PtRu-4-250 °C, and may be due to the lower amount of alloy between Pt–Ru formed.

Cyclic voltammetry of PtRu black prepared with MgO/Pt mass ratio of 4 heat-treated at different temperatures was also investigated (as displayed in Fig. 6). The catalysts showed slightly lower onset potentials for methanol oxidation than that of the commercial PtRu catalyst, indicating an enhanced catalytic activity for methanol oxidation. The peak current densities due to methanol oxidation for PtRu-4-250 °C, PtRu-4-275 °C, PtRu-4-300 °C and

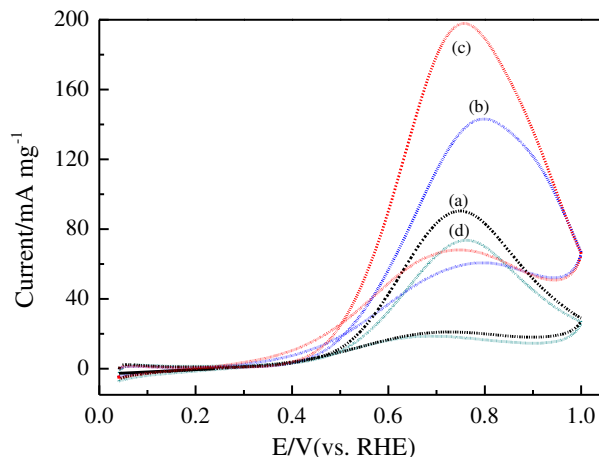


Fig. 5. CVs of (a) PtRu-JM and the PtRu black catalysts heat-treatment at 250 °C with different MgO/Pt mass ratios (b) PtRu-8-250 °C, (c) PtRu-4-250 °C, and (d) PtRu-2-250 °C at a scan rate of 20 mV s⁻¹ in 0.5 M H₂SO₄ + 0.5 M CH₃OH.

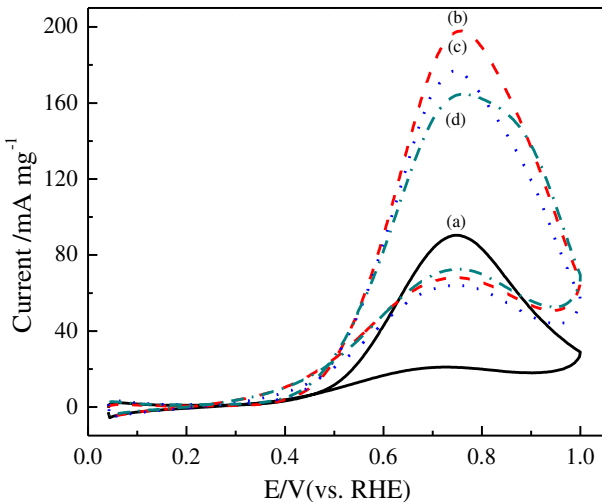


Fig. 6. CVs of the (a) PtRu-JM, (b) PtRu-4-250 °C, (c) PtRu-4-275 °C, and (d) PtRu-4-300 °C at a scan rate of 20 mV s⁻¹ in 0.5 M H₂SO₄ + 0.5 M CH₃OH.

PtRu-JM were 198, 177, 164 and 91 mA mg⁻¹, respectively (see in Table 2). The catalytic activities can therefore be ranked in the order PtRu-JM < PtRu-4-300 °C < PtRu-4-275 °C < PtRu-4-250 °C, indicating that PtRu-4-250 °C is the most active among the catalysts under investigation. As discussed above, the in-house prepared PtRu black catalysts possess similar alloy degree and mean particle size of PtRu black, with MgO/Pt mass ratio of 4, heat-treated at 250 °C, having the smallest particle. Therefore, in the present study, the activity change of methanol oxidation with heat-treatment temperature may be attributed mainly to the particle size effect, as well as partially to change the Pt–Ru alloy content in the catalysts.

We further evaluated the activity and stability of the catalytic electrodes via polarization studies. As described also in one of our earlier papers (see Ref. [19], section 3.3), the electrodes were polarized at 0.35 V/RHE for a period of time. Fig. 7 shows the chronoamperometric (CA) curves for methanol oxidation for in-house prepared PtRu black catalysts and the commercial PtRu catalyst. From Fig. 7A, it was ascertained that the maximum oxidation current density was obtained with the PtRu-4-250 °C catalyst. The activity change for methanol oxidation decreases in the order of PtRu-JM < PtRu-4-250 °C < PtRu-4-275 °C < PtRu-4-300 °C. Also, to examine the possible effect of the heat-treatment temperature of the PtRu black catalysts on its stability for methanol oxidation, essentially the same measurements as detailed in our earlier investigation (section 3.3 of Ref. [19]) normalized current density (i/i_{max}) versus time was plotted as shown in Fig. 7B. We found that the catalytic current density decayed monotonically with time, but at different rates. For 4000 s polarization, methanol oxidation current on the PtRu-JM, PtRu-4-250 °C, PtRu-4-275 °C and PtRu-4-300 °C decreased to 41.18%, 55.55%, 59.50% and 68.96%, respectively. Clearly, such chronoamperometric data indicate that the enhanced stability of the catalysts at evaluated temperatures may be associated with increased alloying.

3.3. DMFC tests

To explore the possible application of the in-house prepared PtRu black catalysts, polarization performance of the passive DMFCs with PtRu-4-y and PtRu-JM as the anode catalysts was shown in Fig. 8. In the low current density region, the DMFCs polarization was primarily attribute to sluggish charge transfer at

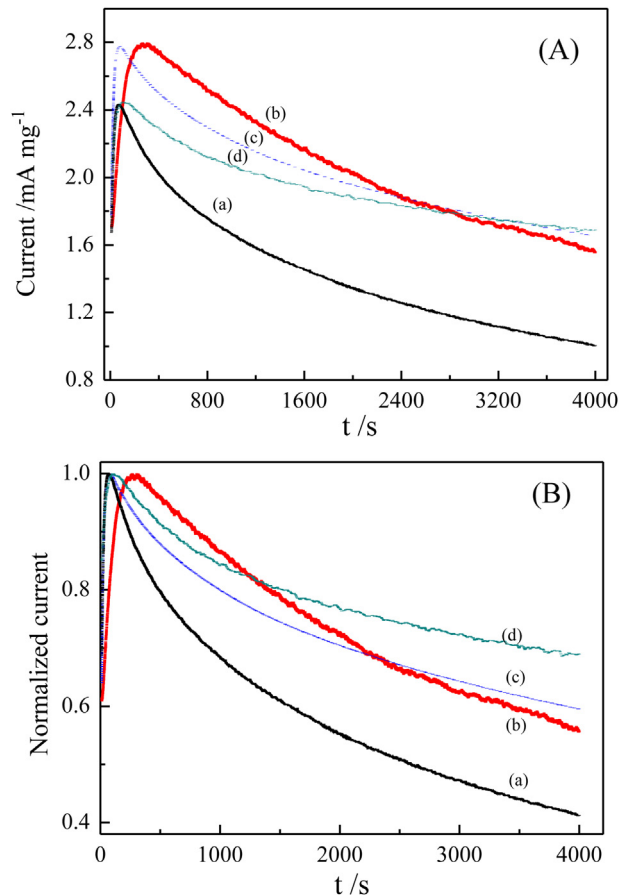


Fig. 7. (A) Chronoamperometric curves of (a) PtRu-JM, (b) PtRu-4-250 °C, (c) PtRu-4-275 °C, and (d) PtRu-4-300 °C in 0.5 M H₂SO₄ + 0.5 M CH₃OH at a given potential of 0.35 V/RHE and (B) their normalized current–time curves.

electrode surface. The current density at 0.5 V [33], which means the activation polarization is mainly affected by activity of the catalyst, was ranked in the order PtRu-JM < PtRu-4-300 °C < PtRu-4-275 °C < PtRu-4-250 °C, indicating more rapid methanol oxidation kinetics on the surface of PtRu-4-250 °C. In addition, the DMFC with PtRu-4-250 °C as anode demonstrated a maximum power

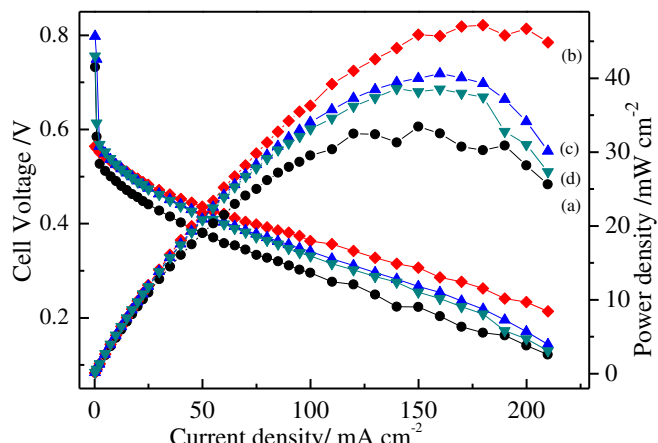


Fig. 8. Polarization curves of the passive DMFCs with (a) PtRu-JM, (b) PtRu-4-250 °C, (c) PtRu-4-275 °C, and (d) PtRu-4-300 °C as anode catalysts and operating with 3 M methanol solution.

density of ca. 47.18 mW cm⁻², which was higher than that with PtRu-4-275 °C (40.60 mW cm⁻²) and with PtRu-4-300 °C (38.59 mW cm⁻²), and much higher than that with the PtRu-JM (33.44 mW cm⁻²). These results again assessed that the PtRu-4-250 °C exhibited the highest electrocatalytic activity toward methanol oxidation which was in good agreement with the conclusion obtained from the CV measurements of Fig. 6.

4. Conclusion

PtRu black catalysts of high alloying degree were synthesized via sacrificial use of a magnesia nanoparticles' support. All in-house prepared PtRu black catalysts have a unique and highly disordered face-centered cubic structure (solid solution). Also, highly uniform nanoparticles and high alloy degrees were obtained and the structure and morphology of catalysts were easily controlled. The in-house prepared PtRu black catalysts were active for CO and methanol oxidation. In addition, the prepared catalysts exhibited a high catalytic activity and good stability for methanol oxidation comparable to the commercial catalysts.

Acknowledgments

We would like to thank the National Basic Research Program of China (973 Program) (2012CB932800); the National Natural Science Foundation of China (21276158); Shanghai Science and Technology Committee (11DZ1200400, 12ZR1431200); and the Knowledge Innovation Engineering of the Chinese Academy of Sciences (12406, 124091231) for support to this work. Also, DLA thanks the U.S. National Science Foundation for support under Cooperative Agreement number HRD-08-33180 for support of this work.

References

- [1] G. Wang, T. Takeguchi, E.N. Muhamad, T. Yamanaka, M. Sadakane, W. Ueda, *J. Electrochem. Soc.* 156 (2009) B1348–B1353.
- [2] C. Bock, C. Paquet, M. Couillard, G.A. Botton, B.R. MacDougall, *J. Am. Chem. Soc.* 126 (2004) 8028–8037.
- [3] Q. Lu, B. Yang, L. Zhuang, J. Lu, *J. Phys. Chem. B* 109 (2005) 1715–1722.
- [4] E.S. Steigerwalt, G.A. Deluga, C.M. Lukehart, *J. Phys. Chem. B* 106 (2002) 760–766.
- [5] Y.S. Wang, S.Y. Yang, S.M. Li, H.W. Tien, S.T. Hsiao, W.H. Liao, C.H. Liu, K.H. Chang, C.C.M. Ma, C.C. Hu, *Electrochim. Acta* 87 (2013) 261–269.
- [6] L.X. Yang, C. Bock, B. MacDougall, J. Park, *J. Appl. Electrochem.* 34 (2004) 427–438.
- [7] W. Xu, R. Si, S.D. Senanayake, J. Llorca, H. Idriss, D. Stacchiola, J.C. Hanson, J.A. Rodriguez, *J. Catal.* 291 (2012) 117–126.
- [8] K.S. Sim, S.M. Lim, H.D. Kwon, S.H. Choi, *J. Nanomater.* 2011 (2011) 1–8.
- [9] X. Ren, *J. Electrochem. Soc.* 143 (1996) L12–L15.
- [10] O.A. Khazova, A.A. Mikhailova, A.M. Skundin, E.K. Tuseeva, A. Havranek, K. Wippermann, *Fuel Cells* 2 (2003) 99–108.
- [11] Y. Chen, Y. Tang, C. Liu, W. Xing, T. Lu, *J. Power Sources* 161 (2006) 470–473.
- [12] D. Chu, S. Gilman, *J. Electrochem. Soc.* 143 (1996) 1685–1690.
- [13] J. Guo, G. Sun, S. Shiguo, Y. Shijou, Y. Weiqian, Q. Jing, Y. Yushan, X. Qin, *J. Power Sources* 168 (2007) 299–306.
- [14] C. Korzeniewski, R. Basnayake, G. Vijayaraghavan, Z. Li, S. Xu, D.J. Casadonte, *Surf. Sci.* 573 (2004) 100–108.
- [15] R. Basnayake, Z. Li, S. Katar, W. Zhou, H. Rivera, E.S. Smotkin, D.J. Casadonte Jr., C. Korzeniewski, *Langmuir* 22 (2006) 10446–10450.
- [16] S. Stoupin, H. Rivera, Z. Li, C.U. Segre, C. Korzeniewski, D.J. Casadonte Jr., H. Inoue, E.S. Smotkin, *Phys. Chem. Chem. Phys.* 10 (2008) 6430–6437.
- [17] H. Yang, C. Coutanceau, J.M. Leger, N. Alonso-Vante, C. Lamy, *J. Electroanal. Chem.* 576 (2005) 305–313.
- [18] H. Yang, W. Vogel, C. Lamy, N. Alonso-Vante, *J. Phys. Chem. B* 108 (2004) 11024–11034.
- [19] J. Liu, J. Cao, Q. Huang, X. Li, Z. Zou, H. Yang, *J. Power Sources* 175 (2008) 159–165.
- [20] A.J. Dickinson, L.P.L. Carrette, J.A. Collins, K.A. Friedrich, U. Stimming, *Electrochim. Acta* 47 (2002) 3733–3739.
- [21] J.C. Calabrese, L.F. Dahl, P. Chini, G. Longoni, S. Martinengo, *J. Am. Chem. Soc.* 96 (1974) 2614–2616.
- [22] G. Longoni, P. Chini, *J. Am. Chem. Soc.* 98 (1976) 7225–7231.
- [23] W. He, M. Chen, Z.Q. Zou, Z.L. Li, X.G. Zhang, S.A. Jin, D.J. You, C. Pak, H. Yang, *Appl. Catal. B* 97 (2010) 347–353.
- [24] W. He, J.Y. Liu, Y.J. Qiao, Z.Q. Zou, X.G. Zhang, D.L. Akins, H. Yang, *J. Power Sources* 195 (2010) 1046–1050.
- [25] X. Li, Q. Huang, Z. Zou, B. Xia, H. Yang, *Electrochim. Acta* 53 (2008) 6662–6667.
- [26] E. Antolini, F. Cardellini, *J. Alloys Compd.* 315 (2001) 118–122.
- [27] Y. Zhang, Q. Huang, Z. Zou, J. Yang, W. Vogel, H. Yang, *J. Phys. Chem. C* 114 (2010) 6860–6868.
- [28] C.J. Corcoran, H. Tavassol, M.A. Rigsby, P.S. Bagus, A. Wieckowski, *J. Power Sources* 195 (2010) 7856–7879.
- [29] X. Li, J. Liu, Q. Huang, W. Vogel, D.L. Akins, H. Yang, *Electrochim. Acta* 56 (2010) 278–284.
- [30] H. Kim, I. Rabelo de Moraes, G. Tremiliosi-Filho, R. Haasch, A. Wieckowski, *Surf. Sci.* 474 (2001) L203–L212.
- [31] P.A. Christensen, J.M. Jin, W.F. Lin, A. Hamnett, *J. Phys. Chem. B* 108 (2004) 3391–3394.
- [32] S.D. Lin, T.C. Hsiao, J.R. Chang, A.S. Lin, *J. Phys. Chem. B* 103 (1999) 97–103.
- [33] M.-S. Kim, B. Fang, N.K. Chaudhari, M. Song, T.-S. Bae, J.-S. Yu, *Electrochim. Acta* 55 (2010) 4543–4550.